Analysis of Omnidirectional Dual-Reflector Antennas with Radomes

Úrsula C. Resende*, Fernando J. S. Moreira, and Odilon M. C. Pereira Filho

*Dept. Electrical Engineering, CEFET-MG, Belo Horizonte, MG, CEP 35510-000, Brazil
Dept. Electronics Engineering, UFMG, Belo Horizonte, MG, CEP 31270-901, Brazil

***Abstract* — We investigate the influence of dielectric radomes on the electromagnetic performance of dual-reflector antennas suited for omnidirectional coverages. The dual-reflector systems are fed by a TEM coaxial horn. Accurate analyses are provided by surface integral equations numerically evaluated by the method of moments, taking into account all electromagnetic couplings among the several antenna elements. The analyses demonstrate that λ/2–window radomes do not significantly influence the antenna behavior across the operation band. But the way the radome is attached to the dual-reflector structure may significantly influence the sidelobe levels of the radiation pattern.**

***Index Terms* — Method of moments, omnidirectional antennas, radomes, reflector antennas.**

I. Introduction

Generally, reflector antennas are used in point-to-point radio links and communications services by satellites demanding point-to-multipoint coverages. These applications are consequence of their high efficiency capability, relative mechanical simplicity, and inherent broadband features and illustrate the use of directive configurations [1]. Reflector antennas can also be used for omnidirectional coverage and their geometrical properties—based on optical principles—make them suited to operate with broadband signals [2]-[8].

In recent years, the growing interest on high-speed wireless communications services, that demand broadband operation, has motivated researches and investigations on more appropriate antenna configurations. Within this scenario, compact reflector antennas may be employed. Single and dual-reflector antennas have been instigated for omnidirecional coverage in the azimuthal plane [2]-[8]. The dual-reflector geometry leads to more compact designs than single reflectors, as the former requires a considerably smaller reflector diameter to achieve the required aperture width for adequate control of the radiation pattern in the elevation plane [8]. Dual-reflector configurations also permit the reduction of the feed return loss by minimizing the subreflector scattering toward the feed aperture [3],[4].

There are four different types of axis-displaced dual-reflector antennas for omnidirectional coverage: OADC (omnidirectional axis-displaced Cassegrain), OADG (Gregorian), OADE (ellipse), and OADH (hyperbola) [2]-[7]. Among them, the OADC and OADE allow the attainment of compact geometries [3]-[6]. These antennas may be designed with a dielectric radome, not only to protect the antenna components from environmental conditions, but also to support the subreflector in place, as illustrated, for example, in Fig. 1. In this case, there is no need for metallic struts for the proper subreflector support and a clear antenna aperture can be obtained, in principle. But still, the presence of a dielectric radome does affect the radiation characteristics of the antenna. Therefore, it is important to investigate and, consequently, understand the deleterious radome effects, especially on the feed return loss and on the sidelobe levels of the antenna radiation pattern [9]-[11].

A variety of methods have been proposed to analyze the radiation characteristics of an antenna covered by a dielectric radome [9]-[16]. As the radomes to be considered in this work are made of homogeneous dielectric materials, the most appropriate and, probably, more accurate analysis tool is that based on surface integral equations numerically evaluated by the method of moments (MoM) technique [17]. The MoM technique provides a full-wave analysis, i.e., it does consider all the electromagnetic coupling among the several antenna components, enabling accurate estimates of the antenna radiation pattern (especially far out sidelobe levels) and feed return loss [17].

In this work OADC and OADE dual-reflector antennas covered by dielectric radomes are investigated. The accurate analysis is based on the electric (EFIE) and magnetic (MFIE) field integral equations, together with the appropriate application of the equivalent principle and the necessary boundary conditions. These integral equations are briefly discussed in sect. II. The resulting system of integral equations is numerically evaluated by MoM technique. All antenna configurations are excited by an omnidirectional TEM coaxial horn. In Sects. III and IV we present the analysis results for the OADC and OADE configurations and discuss the effects of the radome on the antenna radiation characteristics. This work is concluded in Sect. V.

II. Surface Integral Equations

The EFIE and MFIE formulations can be written as:

$$\hat{n} \times \mathbf{E}_i^s(\mathbf{J},\mathbf{M}) + \hat{n} \times \mathbf{E}_i^{inc} = -\mathbf{M}\,, \qquad (1)$$

$$\hat{n} \times \mathbf{H}_i^s(\mathbf{J},\mathbf{M}) + \hat{n} \times \mathbf{H}_i^{inc} = \mathbf{J}\,, \qquad (2)$$

where the indices "*s*'' and "*inc*'' represent the scattered and incident fields, respectively, and i = 1, 2 represent the external and internal media of a homogeneous body of revolution.

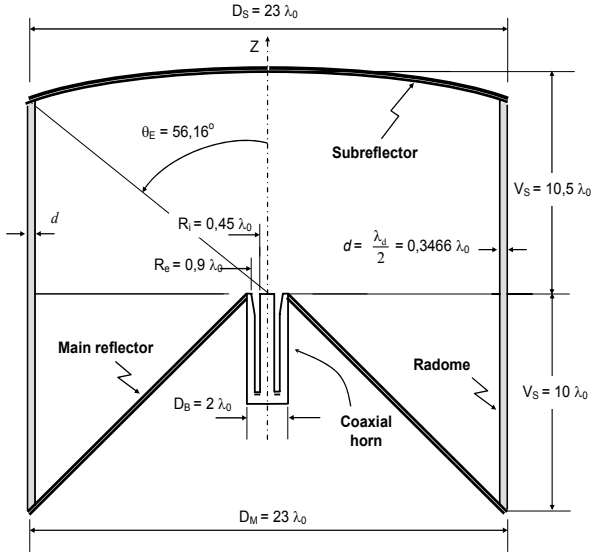

Fig. 1. OADC antenna with dielectric radome.

The equations (1) and (2) may be properly combined to yield formulas suited for the scattering analysis. For perfect electric conductor bodies, the EFIE (1) with **M** = 0 is chosen for open shells (like the reflectors depicted in Fig. 1), while the combined field integral equation (CFIE) is chosen for closed bodies (like the feed structure illustrated in Fig. 1) to avoid spurious solutions related to the internal resonances [17]. The CFIE is a linear combination of (1) and (2), with **M** = 0:

$$\alpha' \,\mathrm{EFIE}_2 + \beta' \,\mathrm{HFIE}_2 \tag{3}$$

where the index i = 2 stresses that the equivalence is valid for the region outside the closed body. For dielectric bodies, like the radome of Fig. 1, (1) and (2) can be combined:

$$\mathrm{EFIE}_1 + \alpha \,\mathrm{EFIE}_2 , \tag{4}$$

$$\mathrm{HFIE}_1 + \beta \,\mathrm{HFIE}_2 , \tag{5}$$

where $\alpha = \varepsilon_1/\varepsilon_2$ and $\beta = \mu_1/\mu_2$ characterize the well-known Müller formulation and $\alpha = \beta = -1$ define the PMCHWT formulation [17].

In the present work the closed conductor and dielectric bodies of the antenna elements are treated by the CFIE and PMCHWT formulations, respectively. The numerical evaluation of the formulations is performed by the MoM technique. Triangular basis functions (TBF) are employed for the equivalent current representation and Galerkin's method is adopted to numerically evaluate the MoM coefficients. All integrals appearing in the MoM full-matrix elements are evaluated by Gaussian quadratures with appropriate singularity treatment [17].

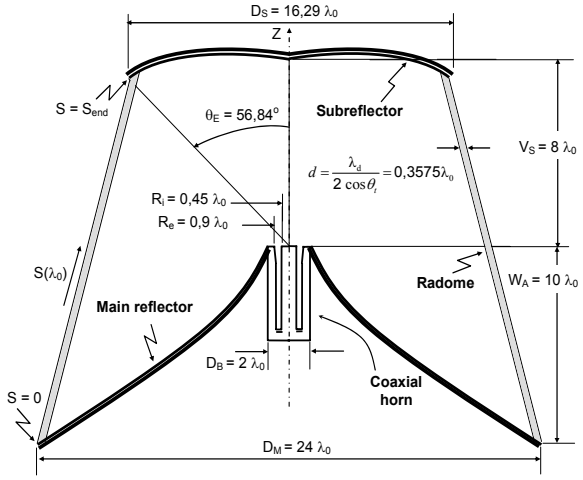

Fig. 2. OADE antenna with dielectric radome: oblique incidence.

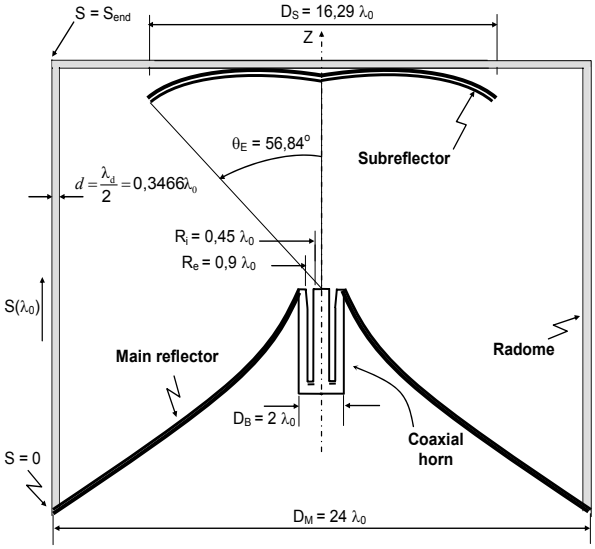

Fig. 3. OADE antenna with dielectric radome: normal incidence.

III. OADC AND OADE OMNIDIRECTIONAL ANTENNA

In this section the electrical performance of OADC and OADE configurations, depicted in Figs. 1—3, are investigated. For the OADE, two kinds of ray incidence over the radome internal surface are considered: oblique and normal, as illustrated in Figs. 2 and 3, respectively. The radome thickness

$$\mathrm{d} = \frac{\lambda_\mathrm{d}}{2\cos\theta_\mathrm{t}} , \tag{6}$$

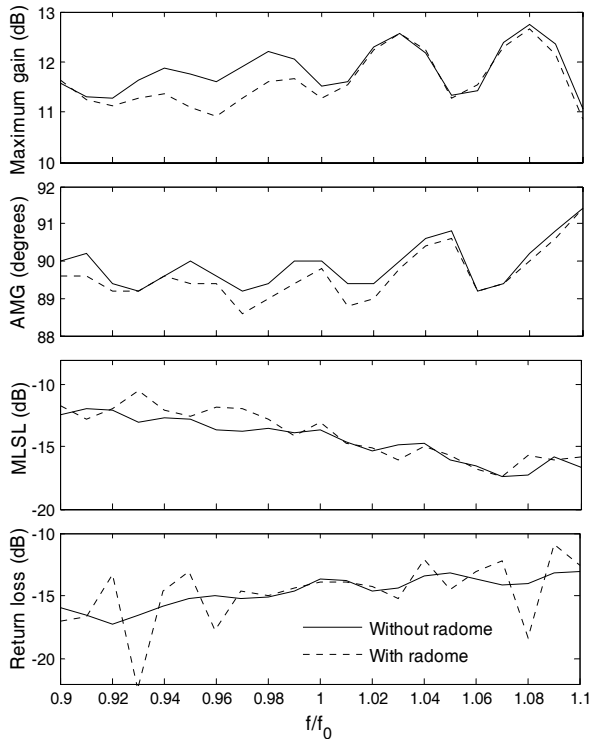

Fig. 4. Electrical parameters for OADC omnidirectional antenna with dielectric radome. a) Maximum gaion. b) AMG. c) MLSL. d) Return loss.

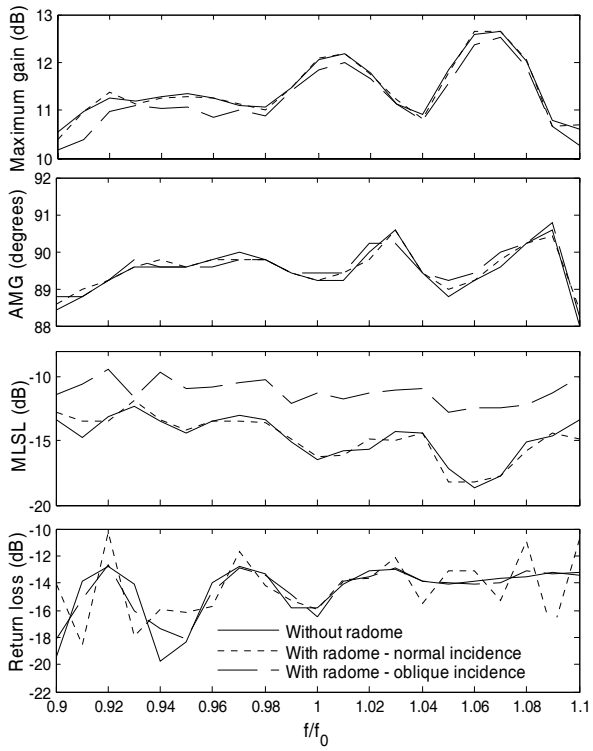

Fig. 5. Electrical parameters for OADE omnidirectional antenna with dielectric radome (normal and oblique incidence). a) Maximum gaion. b) AMG. c) MLSL. d) Return loss.

is chosen for minimal reflection (i.e, the radome is a half-wavelength window), where λ_d is the wavelength in the dielectric and θ_t is the transmission angle inside the dielectric [17]. It is employed a radome with relative permittivity of 2.08. The analyses were conducted for a 20% bandwidth with an arbitrary central frequency (f_0). Figs. 4 and 5 illustrate the maximum gain, the angle where maximum gain occur (AMG), the return loss, and the mean level of secondary lobes (MLSL) obtained from the MoM analyses of the OADC and OADE antennas, respectively. It can be observed that, except for the pattern sidelobe levels and feed return loss, the overall antenna performance is not significantly affected by the radome presence across the operation band. The expected small oscillations present in the results of Figs. 4 and 5 are caused by the coupling among the several antenna components. The radiation patterns of the OADC and OADE antennas at the central frequency (f_0) are depicted in Figs. 6 and 7, respectively. From Fig. 7 one observes an increase of the sidelobe levels for the OADE geometry of Fig. 2 at $\theta \leq 40°$. In order to better understand the causes of such increase in sidelobe level, some case studies are investigated in the next section.

IV. Radome Influence in the Antenna Performance

As can be verified from Figs. 4—7, the electromagnetic performances of the omnidirectional dual-reflector antennas of Figs. 1—3 are not significantly altered by the presence of the radome. Besides an increase of the return-loss oscillations across the operation band, as indicated in Figs. 4(d) and 5(d), the radome is capable of increasing sidelobe levels considerably, as in the case of the OADE antenna of Fig. 2, whose radiation pattern is depicted in Fig. 7. In order to better understand the causes of this increase in sidelobe levels, other OADE configurations where analyzed for different radome inclinations, which are specified by the angle θ_{incl} in Fig. 8. The reflector surfaces and feed structure are still the same of Figs. 2 and 3. Also, one should observe that the OADE configuration of Fig. 8 with $\theta_{incl} = 0°$ is that of Fig. 3. Two other configurations, with $\theta_{incl} = 6.09°$ and 12.04°, were also analyzed by the MoM technique. The radiation patterns obtained in the analysis are illustrated at Fig. 9 at the central frequency (f_0). As one can verify, the radome inclination do not significantly change the antenna radiation pattern. So, the sidelobe increase verified in Fig. 7 at $\theta \leq 40°$ for the OADE configuration of Fig. 2 may be related

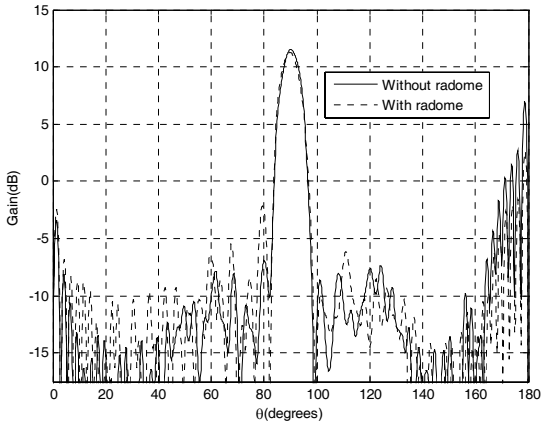

Fig. 6. Radiation patterns: OADC antenna at central frequency.

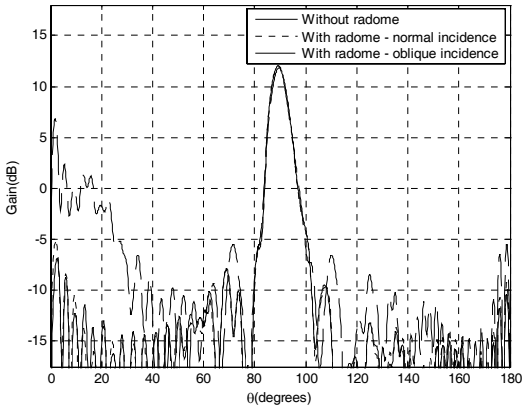

Fig.7. Radiation patterns: OADE antenna at central frequency.

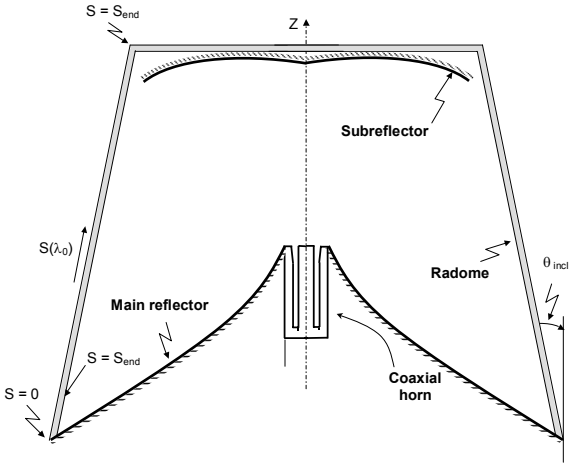

Fig. 8. OADE omnidirectional antenna with dielectric radome for different radome inclinations.

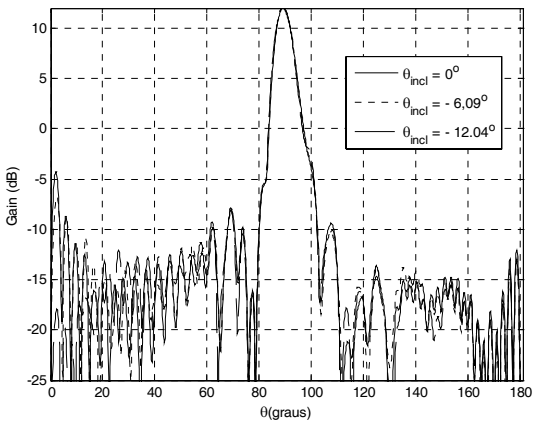

Fig. 9. Radiation patterns: OADE antenna at central frequency for different radome inclinations.

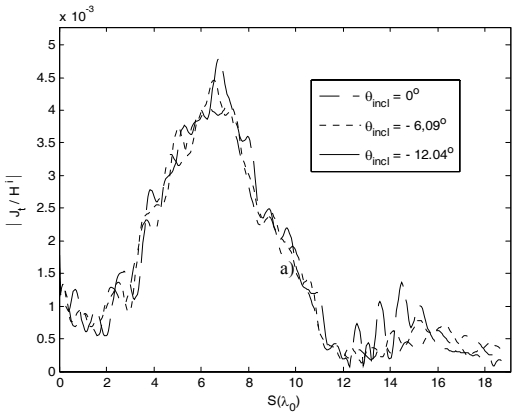

Fig. 10. Surface electrical current in the dielectric radome of OADE antenna of Fig 8.

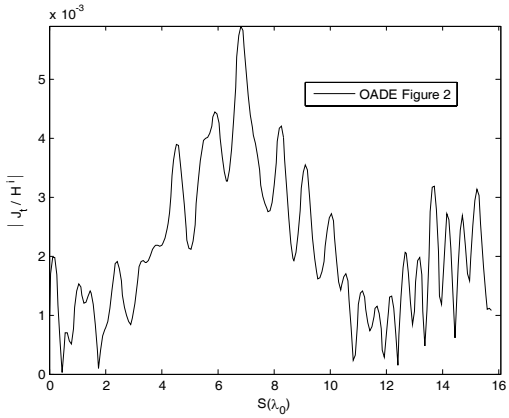

Fig. 11. Surface electrical current in the dielectric radome of OADE antenna of Fig 2.

to the radome attachment at the subreflector rim, which does not occur at the OADE geometries illustrated in Figs. 3 and 8.

For better understanding of the causes of the increase in sidelobe levels, the surface current behavior at the external surface of the radome was investigated. Figs. 10 and 11 shows the current in $\hat{t}$ direction (where $\hat{t}$ is the unit vector tangent to the antenna surfaces in the generatrix curve direction) as function of surface coordinate $S(\lambda_0)$, which vary from $S = 0$ to $S = S_{end}$, for both configurations illustrated in the Figs. 2 and 8. From these results it can be verified that the current presents a much smaller oscillation for the antenna in Fig. 8 than for that in Fig. 2. It is suggested that the increase in sidelobe levels may be related to these current oscillations. This current behavior is not caused by an inaccuracy in the technique used, because the same result was found using more points of integration and more segments to describe the antenna surfaces. So we can conclude that these current oscillations are cased by a considerable stationary wave in side of radome for antenna illustrated at Fig. 2.

V. Conclusion

In this paper OADC and OADE omnidirectional dual-reflector antennas covered by a dielectric radome were investigated. The rigorous analysis was based on electric (EFIE) and magnetic (MFIE) field integral equations, numerically evaluated by the MoM technique. The antenna systems were excited by an omnidirectional TEM coaxial horn. It was verified that the electrical performance of the analyzed antennas was not significantly modified across a 20% operation bandwidth. This fact, at first, enables these antennas configuration to operate in broadband services. It was also verified that when the field incidence upon the radome surface is normal it does not affect the antenna performance. But for oblique incidence case the secondary lobe levels may increase significantly, depending on how it is attached to the antenna.

References

[1] W. V. T. Rusch, "The current state of the reflector antenna art – entering the 1900's," Proc. IEEE, Vol. 80, no. 1, pp 113-126, January 1992.

[2] F. J. S. Moreira and J. R. Bergmann, "Classical axis-displaced dual-reflector antennas for ominidirectional coverage," IEEE Transactions on Antennas and Propagation, vol. 53, no. 9, pp. 2799-2808, September. 2005.

[3] J. R. Bergmann and F. J. S. Moreira, "Simples design equations for ominidirectional axis-displaced dual-reflector antennas," Microwave and Optical Technology Letters, vol. 45, no. 2, pp. 159-163, April 2005.

[4] J. R. Bergmann and F. J. S. Moreira, "An omnidirectional ADE reflector antenna," Microwave and Optical Technology Letters, vol. 40, no. 3, pp. 250-254, February. 2004.

[5] F. J. S. Moreira and J. R. Bergmann, "Axis-displaced dual-reflector antennas for omnidirectional coverage with arbitrary main-beam direction in the elevation plane," IEEE Transactions on Antennas and Propagation, vol. 54, no. 10, pp. 2854-2861, October 2006.

[6] F. J. S. Moreira, A. Prata, Jr. and J. R. Bergmann, "GO Shaping of omnidirectional dual-reflector antennas for a prescribed equi-phase aperture field distribuition," IEEE Antennas and Propagation, vol. 55, no. 1, pp. 99-106, January 2007.

[7] F. F. Dubrovka and A. S. Kim, "A New mathematical model of dual-reflector omnidirectional antennas," Radioelectronics and Communications Systems, Allerton Press, N.Y., USA, vol. 42, no. 6, pp 1-10, 1999.

[8] A. G. Pino, A. M. A. Acuna, and J. O. R. Lopez, "An omnidirectional dual-shaped reflector antenna," Microwave and Optical Technology Letters, vol. 27, no. 5, pp. 371-374, December 2000.

[9] V. B. Yurchenko, A. Altintas, and A. I. Nosich, "Numerical optimization of a cylindrical reflector-in-radome antenna system," IEEE Transactions on Antennas and Propagation, vol. 47, no. 4, pp. 668-673, April 1999.

[10] T. Oguzer, "Analysis of circular reflector antenna covered by concentric dielectric radome," IEEE Transactions on Antennas and Propagation, vol. 49, no. 3, pp. 458-463, March 2001.

[11] O. S. Kim, "Optimization of a dielectric radome for a dual-reflector omnidirectional antenna," MSMW '2OOI Syposium Proceedings. Kharkov, Ukraine, pp. 612-614, June 2001.

[12] J. D. Walton Jr., Radome Engineering Handbook: Design and Principles, New York: Marcel Dekker, 1970.

[13] D. C. F. Wu and R. C. Rudduck, "Plane wave spectrum-surface integration technique for radome analysis," IEEE Transactions on Antennas and Propagation, vol. 22, pp. 497-500, May 1974.

[14] R. K. Gordon an R. M. Mittra, "Finite element analysis of axisymmetric radomes," IEEE Transactions on Antennas and Propagation, vol. 41, pp. 975-981, July 1993.

[15] C. C. Lu, "Dielectric radome analysis using multilevel fast multiple algorithm," Antennas and Propagation Society International Symposium, pp 730-733, 2001.

[16] O. S. Kim, "Optimization of a dielectric radome for a dual-reflector omnidirectional antenna," MSMW 2001, Symposium Proceedings, Kharkov, Ukranie, June 2001.

[17] U. C. Resende, Análise de antenas refletoras circularmente simétricas com a presença de corpos dielétricos, Doctorate Thesis, Dept. of Electronics Engineering, UFMG, Minas Geriais, Brazil, May 2007.